







Proceedings Article

# Model-based calibration and image reconstruction with immobilized nanoparticles

Hannes Albers <sup>a</sup> · Florian Thieben <sup>b,c</sup> · Marija Boberg <sup>b,c</sup> · Konrad Scheffler <sup>b,c</sup> · Tobias Knopp <sup>b,c</sup> · Tobias Kluth <sup>a</sup>

<sup>a</sup>Center for Industrial Mathematics, University of Bremen, Bremen, Germany

<sup>b</sup>Section for Biomedical Imaging, University Medical Center Hamburg-Eppendorf, Hamburg, Germany

<sup>c</sup>Institute for Biomedical Imaging, Hamburg University of Technology, Hamburg, Germany

\*Corresponding author, email: [halbers@uni-bremen.de](mailto:halbers@uni-bremen.de)

© 2023 Albers *et al.*; licensee Infinite Science Publishing GmbH

This is an Open Access article distributed under the terms of the Creative Commons Attribution License (<http://creativecommons.org/licenses/by/4.0>), which permits unrestricted use, distribution, and reproduction in any medium, provided the original work is properly cited.

## Abstract

The model-based reconstruction problem is still one of the key challenges in magnetic particle imaging (MPI) when using multi-dimensional Lissajous-type excitations. One aspect, which is often highlighted in the literature, is the magnetization behavior of the magnetic nanoparticles in fluids. Another aspect, which is at least as important as the particle model itself but sometimes treated less prominently, is a very careful calibration of the model input, respectively the scanner parameters such as analog filter and applied magnetic fields. The careful consideration of both aspects is the essential requirement for a proper solution to the model-based problem. In the present work we combine previously calibrated scanner components with mono- and polydisperse particle models for immobilized nanoparticles to derive a model-based system function and an calibration routine exploiting applied magnetic field generalizability. It is experimentally validated on the Bruker preclinical MPI system using 2D Lissajous trajectories.

## 1. Introduction

Proper modeling of the concentration-to-voltage mapping in magnetic particle imaging (MPI) is still one of the open key challenges particularly for multi-dimensional excitation patterns such as Lissajous-type ones. The solution up to now is a time-consuming calibration of the entire system matrix, which also suffers from limited generalizability and spatial resolution.

To properly describe this mapping, the dynamic behavior of the magnetic nanoparticles' (MNPs') magnetic moments, as well as the involved scanner parameters such as the applied magnetic field, the analog filter, and the sensitivity profile of the receive coils, need to be accurately known. For the particle model, two well-known mechanisms need to be taken into account, namely Brownian and Néel rotation [1], which reduces to only Néel rotation if the MNPs are immobilized [2, 3].

The independent calibration of the scanner components is one essential prerequisite for a proper modeling

of the system function. For example, in earlier works [4, 5] the entire analog filter has been fitted to the particle delta sample measurements. As a consequence, the particle model and scanner parameters are mixed and conclusions on the suitability of the particle model and the involved parameters are not possible. Besides exact knowledge of the involved magnetic fields, a necessary requirement for particle model parameter interpretability is a precise MPI receive path calibration, which can be carried out by measuring the transfer function of the analog filter. In [6], it was shown that this transfer function enables transforming the system-specific receive signal into the magnetization domain. In addition, the prior determination of scanner parameters, which is independent of any tracer material, is an essential prerequisite to obtain generalizability of the particle model with respect to scanner parameters such as the applied field. Under these circumstances the scanner's functionality becomes similar to a multi-dimensional magnetic particle spectrometer, which is able to generate multi-dimensional

Lissajous-type excitations with arbitrary offset fields [7].

In the present work we combine the following steps: First, for the calibration of the scanner's applied magnetic field, receive coil sensitivities, and analog filters we exploit measurement techniques being independent of any tracer material containing MNPs. This is done on the Bruker preclinical MPI system. Second, for the particle magnetization model we focus on the immobilized case allowing for using the simpler Néel model with uniaxial anisotropy. Here, we consider monodisperse as well as polydisperse tracer models taking into account particle diameter and anisotropy constant. Remaining unknown particle model parameters are determined in another calibration routine exploiting 1D excitations on the Bruker preclinical MPI system. Third, fully measured and model-based system matrices for 2D Lissajous-type excitations are used for image reconstruction of a capillary phantom on the Bruker preclinical system.

## II. Methods and materials

The setting of a general MPI imaging experiment reads as follows: Let  $\Omega \subset \mathbb{R}^3$  be the field-of-view containing MNPs. A voltage induced by the MNPs' in a receive coil with sensitivity profile  $p : \mathbb{R}^3 \rightarrow \mathbb{R}^3$  in  $\text{m}^{-1}$  after applying an analog filter  $a : \mathbb{R} \rightarrow \mathbb{R}$  in Hz is approximately given by

$$\tilde{v}_M(t) = - \left( a * \mu_0 \int_{\Omega} c(r) p(r)^T \frac{\partial}{\partial t} \tilde{m}(r, \cdot) dr \right) (t) \quad (1)$$

in V where  $\mu_0$  is the vacuum permeability in  $\text{kgmA}^{-2} \text{s}^{-2}$ ,  $c : \Omega \rightarrow \mathbb{R}_0^+$  in  $\text{molL}^{-1}$  is the concentration of the magnetic nanoparticles and  $\tilde{m} : \mathbb{R}^3 \times [0, T] \rightarrow \mathbb{R}^3$  in  $10^{-3} \text{Am}^2 \text{mol}^{-1}$  is the molar mean magnetic moment. The mean magnetic moment  $\tilde{m}(r, t)$  is given by a *particle model* and it depends on the applied magnetic field  $H : \mathbb{R}^3 \times [0, T] \rightarrow \mathbb{R}^3$  in  $\text{T} \mu_0^{-1}$ . The applied field, the analog filter, and the sensitivity profile are the *scanner parameters*.

### II.I. Scanner parameter calibration

The identification of all involved scanner parameters is done independent of any particle system. To gain precise information of the applied magnetic fields, the dynamic drive field (resp. sensitivity profile) and the selection field are represented by spherical harmonic expansions. These are obtained by measuring an appropriate spherical t-design providing exact information of the fields inside the measured sphere [8, 9]. Furthermore, MPI receive path calibration is performed to acquire the frequency dependent transfer function [6].

### II.II. Particle models

In the model equation (1) we need a proper model for the mean magnetic moment  $\tilde{m}$  of the ensemble of nanopar-

ticles. Here we use the Fokker-Planck (FP) equation approach for the Landau-Lifshitz-Gilbert equation as described in [3]. The simulations are performed with a finite volume method as described in [10]. The model depends on the particle diameter  $D$  and the anisotropy constant  $K^{\text{anis}}$  which substantially influence the behavior. We simulate  $\tilde{m}$  for different values of  $D$  and  $K^{\text{anis}}$ , and we take a uniform distribution of easy axes into account. The result using the field  $H$  is denoted by  $\tilde{m}_{\text{FP-anis};D,K^{\text{anis}}}$ .

### II.III. Particle model calibration

To obtain a modeled system matrix suitable for image reconstruction, we need to identify two types of unknowns. The first type of unknown concerns measurement inaccuracies which are not yet included in the measured analog filter, in particular, a global scale factor as well as a global time shift: in time domain, we consider  $\tilde{m}_{\text{FP-anis};D,K^{\text{anis}}}(t) \approx \beta \tilde{m}_{\text{calib}}(t - \Delta t)$ , where  $\tilde{m}_{\text{calib}}$  denotes the measurement after being corrected for the measured transfer function.  $\beta$  and  $\Delta t$  are fitted to a pre-selected small number of calibration measurements. Importantly, a full system matrix measurement is not necessary for this procedure. In fact, one measurement at the center of the field-of-view would be sufficient.

The second unknown parameters are the particle properties  $D$  and  $K^{\text{anis}}$  or their distributions in the polydisperse case. Assuming monodisperse tracers, we choose the parameter from a dictionary that has the smallest  $\ell^2$ -distance to a full system matrix measurement. For the polydisperse case, we consider the full dictionary over  $D$  and  $K^{\text{anis}}$  and perform a nonnegative least squares fit for

$$\tilde{m}_{\text{FP-anis};\text{poly}} = \sum_D \sum_{K^{\text{anis}}} w_{D,K^{\text{anis}}} \tilde{m}_{\text{FP-anis};D,K^{\text{anis}}} \quad (2)$$

to obtain weights  $w_{D,K^{\text{anis}}} \geq 0$  such that  $\tilde{m}_{\text{FP-anis};\text{poly}}$  is closest to  $\tilde{m}_{\text{calib}}$ . In this case, the fitting of  $(\beta, \Delta t)$  and of the weights is alternately refined up to convergence. Exploiting the generalizability with respect to the applied magnetic fields of the proposed approach, we can reduce the computational overhead. The full dictionary with respect to  $(D, K^{\text{anis}})$  has been computed for a 1D excitation only. After obtaining  $w_{D,K^{\text{anis}}}$ , 2D system matrices are simulated for only those  $(D, K^{\text{anis}})$  that were associated with nonzero weights.

### II.IV. Image reconstruction

For image reconstruction, a background subtraction using convex combinations of background measurements and diagonal whitening of the complex-valued system matrix is performed (see, e.g., [11]). The background measurements are also added to the system matrix as scaled additional columns with positive and negative sign to reduce the influence of noise during reconstruction [12]. No frequency selection is performed except for

applying a band pass filter. Then, the reconstruction is carried out using the constrained regularized Kaczmarz method [13] to obtain real-valued positive coefficients.

### III. Experiments

The scanner parameter calibration of the Bruker preclinical system has been performed according to Section II.I. The magnetic fields are measured at 36 positions of a spherical 8-design yielding polynomials of degree 4. For the selection field, a 3D Hall probe was placed at each position [8] while a 3D calibration coil was used to measure the drive field [9]. For the receive-path calibration, a 3D calibration-coil setup is utilized. A defined signal analog to a magnetic moment signal was generated per direction and the system-specific receive signal was measured [6].

2D system matrices were measured on a  $17 \times 15$  grid, using a delta sample of  $2 \times 2 \times 2 \text{ mm}^3$  filled with immobilized perimag (micromod Partikeltechnologie GmbH, Rostock, Germany) at a concentration of  $10 \text{ mg}_{\text{Fe}} \text{ mL}^{-1}$ . A gradient strength of  $(-1, -1, 2) \text{ T m}^{-1}$  and a 1D excitation in  $x$ -direction as well as a 2D Lissajous-type excitation in  $xy$ -direction were used on the Bruker preclinical system. These fully measured system matrices ( $x$ - and  $y$ -receive channel) represent a reference for quantitative comparison as well as for the image reconstruction. For the latter we measured a capillary phantom with a diameter of 2.5 mm and a length of 12 mm placed from the origin along the positive  $y$ -axis averaged over 200 frames.

In the monodisperse particle model calibration  $(\Delta t, \beta)$  estimation is performed with five measurements around the origin for improved stability against noise. 1D excitation in the applied field is used. Due to the high dimensionality of the weighting in the polydisperse case, the fully measured system matrix of 1D excitation is used to obtain  $(\Delta t, \beta, w_{D, K^{\text{anis}}})$ .

The image reconstruction according to Section II.IV uses a bandpass of the range [90 kHz, 625 kHz]. The algorithm uses 1000 iterations ( $\lambda = 2 \cdot 10^{-5}$ , normalized via operator norm). For the mono- and polydisperse model-based case, the system matrices are generated for the 2D Lissajous-type excitation of the Bruker preclinical system using the parameters determined by the previously described calibration procedure using 1D excitations.

### IV. Results

The obtained weight distribution for the polydisperse model is displayed in Figure 1. The weights are localized around diameters of 15-20 nm and anisotropy constants of 0-2000  $\text{J/m}^3$ . Since we are dealing with non-aligned immobilized tracers, we expect particle anisotropy to have only a small effect, which is reflected in the obtained distribution. The relative deviation [3, eq. (22)] to the measured system matrix for 2D excitation is 0.2444 in

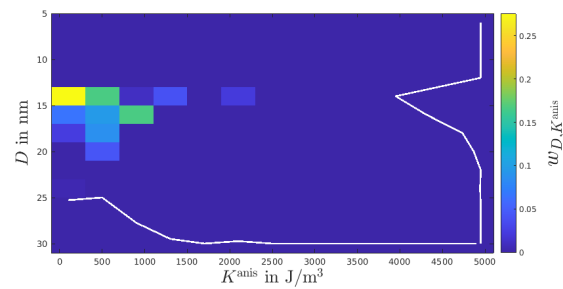


**Figure 1:** Weights obtained with the polydisperse model. The respective marginal distributions are displayed in white at the edges.

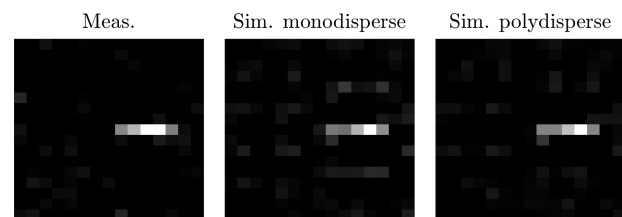


**Figure 2:** Image reconstructions of a capillary phantom with the measured system matrix and the monodisperse and polydisperse Fokker-Planck models.

the mono- and 0.2416 in the polydisperse case on mixing orders up to order 5 contained in the band limit.

In Figure 2, a reconstruction of a capillary phantom is shown for the fully calibrated system matrix, the simulated monodisperse model, and the simulated polydisperse model with the weighting shown in Figure 1. While the monodisperse model still produces a slightly noisier image than the polydisperse model, which is still of inferior quality to the fully calibrated approach, both simulated approaches lead to a good quality reconstruction.

### V. Discussion and outlook

The results illustrate that the amount of necessary calibration effort can be reduced by using 1D excitation for the particle model calibration. In addition, the generalization of the fitted model to 2D Lissajous-type excitation has been investigated in the context of image reconstruction. In the monodisperse model the number of required calibration measurements might be further reduced to one to five delta sample measurements for  $(D, K^{\text{anis}})$  estimation which remains future research. In the polydisperse model the number of required calibration measurements is still an open question. Due to the high dimensionality of the weighting function, stability aspects and the ill-posedness of the underlying problem needs to be taken into account. An investigation of the trade-off between number of calibration measurements and model-based a priori information (e.g., assuming

a log-Gaussian particle diameter distribution) is highly desirable for future work.

The scanner parameters are calibrated, which needs to be done only once in general. The influences of aging and component replacements need to be taken into account. Typical time intervals for a re-calibration of the scanner parameters are an open question. The advantage of the proposed calibration method is that the obtained particle model parameters can be re-used in principle. It might become necessary to adjust time-shift and global scaling.

The explicit distinction between scanner parameters and particle model parameters in the calibration has several advantages and paves the way for further model-based calibration methods: (i) *Generalization with respect to particle models can be realized immediately*: Particle model replacements are immediately possible and future work includes considering equilibrium models (Langevin function, uniaxial anisotropy [14]) when considering immobilized nanoparticles and the fluid case in general. (ii) *Generalization with respect to applied magnetic fields*: In the present work we used 1D excitation for calibration and 2D Lissajous-type excitation for image reconstruction. The extension to the 3D Lissajous-type case is straight forward. (iii) *Generalization with respect to calibration device*: In the present work we used the Bruker preclinical system for the purpose of both calibration and imaging. The proposed routine opens the way for particle models being calibrated differently, e.g., on an MPS system [7].

Physical interpretability of the determined particle model parameters is always a delicate issue as they need to be interpreted carefully taking into account the overall context like accuracy of scanner parameters, suitability/design of particle model, used fitting algorithm, a priori information, etc.. The experimental determination of all scanner parameters independent of the involved MNPs can be seen as one step towards an improved interpretability of the particle model parameters.

A comparison to existing model-based calibration procedures is an open research question but it also requires a careful design as scanner parameters and particle model parameters might be mixed in existing approaches such as fitting the transfer function of the analog filter to MNP's measurements [4]. In the proposed method one might include an additional convolution kernel in the particle model (e.g., similar as in [15]) which is determined simultaneously. This is an interesting extension of [4] to further study the trade-off between number of calibration measurements and degrees of freedom. For the polydisperse case this requires more sophisticated methods for parameter identification.

In sum, the potential extensions and further investigation of advantages of model-based representations such as refined spatial resolution remain future work.

## Author's statement

Authors state no conflict of interest.

## Acknowledgments

H. Albers and T. Kluth acknowledge funding by the German Research Foundation (DFG) - project 426078691.

## References

- [1] W. T. Coffey, P. J. Clegg, and Y. U. P. Kalmykov, On the theory of debye and néel relaxation of single domain ferromagnetic particles, in *Advances in Chemical Physics*. John Wiley & Sons, Inc., 1992, 263–464, ISBN: 9780470141410. doi:[10.1002/9780470141410.ch5](https://doi.org/10.1002/9780470141410.ch5).
- [2] S. A. Shah, D. B. Reeves, R. M. Ferguson, J. B. Weaver, and K. M. Krishnan. Mixed brownian alignment and néel rotations in superparamagnetic iron oxide nanoparticle suspensions driven by an ac field. *Phys. Rev. B*, 92:094438, 9 2015, doi:[10.1103/PhysRevB.92.094438](https://doi.org/10.1103/PhysRevB.92.094438).
- [3] H. Albers, T. Knopp, M. Möddel, M. Boberg, and T. Kluth. Modeling the magnetization dynamics for large ensembles of immobilized magnetic nanoparticles in multi-dimensional magnetic particle imaging. *Journal of Magnetism and Magnetic Materials*, 543:168534, 2022, doi:<https://doi.org/10.1016/j.jmmm.2021.168534>.
- [4] T. Knopp, S. Biederer, T. F. Sattel, J. Rahmer, J. Weizenecker, B. Gleich, J. Borgert, and T. M. Buzug. 2D model-based reconstruction for magnetic particle imaging. *Medical Physics*, 37(2):485–491, 2010.
- [5] T. Kluth and P. Maass. Model uncertainty in magnetic particle imaging: Nonlinear problem formulation and model-based sparse reconstruction. *International Journal on Magnetic Particle Imaging*, 3(2):ID 1707004, 10 pages, 2017.
- [6] F. Thieben, T. Knopp, M. Boberg, F. Foerger, M. Graeser, and M. Möddel. On the receive path calibration of magnetic particle imaging systems. *IEEE Transactions on Instrumentation and Measurement*, 72:1–15, 2023, doi:[10.1109/TIM.2022.3219461](https://doi.org/10.1109/TIM.2022.3219461).
- [7] A. von Gladiss, M. Graeser, A. Behrends, X. Chen, and T. M. Buzug. Efficient hybrid 3d system calibration for magnetic particle imaging systems using a dedicated device. *Scientific reports*, 10(1):1–12, 2020.
- [8] M. Boberg, T. Knopp, and M. Möddel. Analysis and comparison of magnetic fields in MPI using spherical harmonic expansions. *8th International Workshop on Magnetic Particle Imaging (IWMPi 2018)*, pp. 159–160, 2018, inproceedings.
- [9] F. Thieben, M. Boberg, M. Gräser, and T. Knopp. Efficient 3d drive-field characterization for magnetic particle imaging systems. *International journal on magnetic particle imaging*, 8(1, Suppl 1), 2022.
- [10] H. Albers, T. Kluth, and T. Knopp. Simulating magnetization dynamics of large ensembles of single domain nanoparticles: Numerical study of Brown/Néel dynamics and parameter identification problems in magnetic particle imaging. *Journal of Magnetism and Magnetic Materials*, 541:168508, 2022, doi:<https://doi.org/10.1016/j.jmmm.2021.168508>.
- [11] T. Kluth and B. Jin. Enhanced reconstruction in magnetic particle imaging by whitening and randomized SVD approximation. *Physics in Medicine & Biology*, 64(12):125026, 2019, doi:[10.1088/1361-6560/ab1a4f](https://doi.org/10.1088/1361-6560/ab1a4f).
- [12] T. Knopp, M. Grosser, M. Graeser, T. Gerkmann, and M. Möddel. Efficient joint estimation of tracer distribution and background signals in magnetic particle imaging using a dictionary approach. *IEEE transactions on medical imaging*, 40(12):3568–3579, 2021.

- [13] A. Dax. On row relaxation methods for large constrained least squares problems. *SIAM J. Sci. Comput.*, 14(3):570–584, 1993, doi:[10.1137/0914036](https://doi.org/10.1137/0914036).
- [14] H. Albers and T. Kluth. Immobilized nanoparticles with uniaxial anisotropy in multi-dimensional lissajous-type excitation: An equilibrium model approach. *International Journal on Magnetic Particle Imaging*, 8(1 Suppl. 1):ID 2203048, 4 pages, 2022.
- [15] L. R. Croft, P. W. Goodwill, and S. M. Conolly. Relaxation in x-space magnetic particle imaging. *IEEE Transactions on Medical Imaging*, 31(12):2335–2342, 2012.